Article Type: Research

OPEN ACCESS

Evaluation of High-Risk Dynamic Zones Caused by Kinematic Brittle Deformation in Northeastern Kerman

Anis Akbarzadeh[1], Shahbaz Radfar[1], Shahram Shafiei Bafti[1,*]

[1]Department of Geology, Shahid Bahonar University of Kerman, Kerman 7616913439, Iran
*Corresponding author: shafiei_shahram@uk.ac.ir

Received: 10 August 2024 / Accepted: 11 October 2024 / Published: 12 December 2024
© The Author(s) 2024

***Abstract*:** This study evaluates high-risk dynamic zones in northeastern Kerman, focusing on the effects of kinematic brittle deformation and their correlation with recorded earthquakes. The region is tectonically active, influenced by major fault systems that contribute to seismic hazards and surface deformation. Identifying these hazardous zones is crucial for risk assessment, infrastructure development, and disaster management. The research integrates geological surveys, remote sensing techniques, and seismic data analysis to assess fault dynamics, lithological characteristics, and historical earthquake occurrences. High-resolution Digital Elevation Models (DEMs) and satellite imagery are employed to map structural discontinuities and deformation patterns. Additionally, seismic records and fault activity data are analyzed to determine the relationship between brittle deformation zones and earthquake distribution. Findings indicate that areas with intense brittle deformation align with active fault zones, making them highly susceptible to seismic hazards. The study reveals that northeastern Kerman experiences frequent moderate-to-strong earthquakes, with significant deformation occurring along major thrust and strike-slip faults. These deformations increase the likelihood of future seismic activity and ground instability. The results provide valuable insights for urban planners, engineers, and policymakers to enhance seismic hazard mitigation strategies. By identifying high-risk zones, the study contributes to informed decision-making for infrastructure planning, land-use management, and disaster preparedness. Future research should focus on integrating machine learning models with geophysical data to improve earthquake prediction accuracy and hazard assessments in tectonically active regions.

Keywords: Seismic hazard, Brittle deformation, Earthquake susceptibility, Fault dynamics, Northeastern Kerman.

I. INTRODUCTION

Faults are fractures in the Earth's crust along which significant displacement has occurred due to tectonic forces (Brideau et al., 2009). These structures play a key role in shaping the Earth's surface, influencing seismic activity, and contributing to landscape evolution (Paronuzzi & Bolla, 2015). Faults are formed in response to stress generated by plate movements, which result in deformation processes ranging from minor fractures to large-scale fault systems (Chigira, 1992). Understanding faults and their mechanisms is essential for assessing seismic hazards, predicting earthquake risks, and implementing effective land-use planning strategies in tectonically active regions (Schultz, 1996).

Faults are classified based on the nature of displacement and the stress regime that governs their formation (Atkinson, 2015). The three primary types of faults are normal faults, reverse (or thrust) faults, and strike-slip faults. Normal faults occur under extensional stress, where the hanging wall moves downward relative to the footwall, typically forming in divergent plate boundaries. Reverse faults result from compressional forces, causing the hanging wall to move upward relative to the footwall, commonly found in convergent plate settings. Strike-slip faults, such as the San Andreas Fault, involve lateral movement along fault planes due to horizontal shear stress, often occurring at transform boundaries (Torabi & Berg, 2011). Fault movement is governed by stress conditions within the Earth's crust (Killick, 2003). These stresses, categorized into compressional, extensional, and shear stresses, dictate how faults behave. Compressional stress leads to reverse and thrust faulting, forming mountainous regions like the Himalayas (Bell, 2007). Extensional stress results in normal faulting, often seen in rift valleys such as the East African Rift. Shear stress causes strike-slip faulting, which is prevalent in transform fault systems (Fasching & Vanek, 2011). The movement along these faults generates seismic energy that propagates as earthquakes (Blyth & De Freitas, 2017).

A fault consists of several structural components, including the fault plane, fault trace, hanging wall, footwall, and fault zone. The fault plane is the surface along which displacement occurs, while the fault trace represents the intersection of the fault with the Earth's surface (Riedmüller et al., 2001). The hanging wall refers to the block of rock above the fault plane, and the footwall is the block below (Avar & Hudyma, 2019). In large-scale fault zones, multiple fault strands, fractures, and deformation bands

contribute to complex fault networks that accommodate tectonic movements (Stead & Wolter, 2015). Active faults are responsible for most of the world's earthquakes, as they release accumulated stress when slip occurs (Mandl, 1999). Earthquakes generated by fault movement vary in magnitude, depth, and frequency depending on the fault type and tectonic setting (Harris, 2017). Faults with high slip rates and significant accumulated strain pose the greatest seismic hazard (Krinitzsky, 2002). Seismologists monitor fault activity using geodetic techniques, GPS measurements, and seismic records to assess the potential for future earthquakes (Ulusay et al., 2002). Tectonic settings play a fundamental role in fault formation and evolution. At divergent boundaries, normal faults accommodate crustal extension, forming mid-ocean ridges and continental rift systems. Convergent boundaries host reverse and thrust faults, where subduction zones and continental collisions generate compressional stress. Transform boundaries are characterized by strike-slip faults, which facilitate lateral displacement between tectonic plates. Each tectonic environment exhibits unique faulting patterns and deformation styles (Scawthorn & Chen, 2002).

Faults evolve over geological timescales, influenced by factors such as lithology, temperature, pressure, and regional stress fields (Krinitzsky, 2002). Some faults remain active for millions of years, accumulating strain and producing recurrent earthquakes (Avar & Hudyma, 2019). Others may become inactive due to changes in stress conditions or tectonic reorganization (Scawthorn & Chen, 2002). The study of ancient fault systems provides insights into past tectonic processes and helps predict future fault behavior (Ulusay et al., 2002). Faults pose significant risks to human settlements, infrastructure, and natural environments (Hencher, 2013). Ground shaking, surface rupture, landslides, and secondary hazards such as tsunamis can result from fault movement (Lin et al., 2021). Understanding fault behavior is critical for earthquake-resistant construction, early warning systems, and disaster preparedness (Bird and Bommer, 2004). Engineers and geologists collaborate to develop building codes and zoning regulations that minimize seismic risks in fault-prone areas (Scawthorn & Chen, 2002).

Advancements in remote sensing and Geographic Information Systems (GIS) have revolutionized fault mapping and hazard assessment. Satellite imagery, LiDAR, and InSAR (Interferometric Synthetic Aperture Radar) enable detailed analysis of fault structures, displacement patterns, and surface deformation (Deligiannakis et al., 2018; Mehrabi et al., 2021). These technologies enhance our ability to monitor fault activity, predict seismic hazards, and plan for sustainable development in tectonically active regions (Zhang et al., 2018). The study of faults and their associated seismic hazards is crucial for understanding earthquake risks and mitigating potential disasters in urban areas (Liu et al., 2012). Faults influence ground stability, infrastructure integrity, and land-use planning, making them a key factor in urban development strategies (Ahmad et al., 2017). By identifying active fault zones and assessing seismic risks, decision-makers can implement policies that enhance public safety and minimize the impact of earthquakes on cities and communities (Hashemi et al., 2011). Such studies provide essential data for designing earthquake-resistant structures, optimizing land-use planning, and improving early warning systems (Scawthorn & Chen, 2002). One of the major advantages of fault studies is their contribution to disaster risk reduction (Ahmadi & Pekkan, 2011). By mapping active fault lines, geologists and engineers can identify high-risk zones where urban expansion should be carefully managed (Karimzadeh et al., 2014). This knowledge allows planners to establish construction regulations that prevent development in hazardous areas, reducing potential damage and casualties (Krinitzsky, 2002). Additionally, seismic hazard assessments inform emergency response strategies, ensuring that cities are better prepared for potential earthquakes through improved infrastructure resilience and effective evacuation plans (Stead & Wolter, 2015).

Despite these benefits, fault studies also face several limitations. The complexity of fault behavior, variations in seismic activity, and uncertainties in earthquake prediction pose significant challenges (Barreca et al., 2013). While modern remote sensing and geophysical techniques have improved fault mapping, predicting the exact time, location, and magnitude of an earthquake remains highly uncertain (Rodríguez-Peces et al., 2014). Additionally, implementing fault-based urban planning requires strong governance, financial investment, and public awareness (Lin & Tung, 2004), which may not always be feasible in rapidly expanding cities with limited resources (Rahman et al., 2015). Moreover, balancing urban development with seismic risk mitigation is a significant challenge (Rodríguez-Peces et al., 2014). Many cities experience rapid population growth and increasing infrastructure demands, making it difficult to restrict development in high-risk areas (Avar & Hudyma, 2019). Retrofitting existing buildings and enforcing strict building codes require substantial funding and long-term planning (Mandl, 1999). Public resistance to relocation from hazard-prone zones also complicates the implementation of seismic risk management strategies (Scawthorn & Chen, 2002). Therefore, integrating fault studies into urban development requires a multidisciplinary approach involving geologists, engineers, policymakers, and community (Torabi & Berg, 2011). Also, the continuous advancement of geospatial technology, machine learning, and real-time monitoring systems is improving our ability to assess seismic risks more accurately (Rouet-Leduc et al., 2017). With better data integration and proactive policies, cities can enhance their resilience against earthquakes while maintaining sustainable development (Tan et al., 2021). Investing in research, infrastructure reinforcement, and public education is essential for minimizing the impact of seismic hazards and ensuring safer urban environments (Hulbert et al., 2019). Northeastern Kerman is a tectonically active region with a history of significant earthquakes due to the presence of major fault systems. Understanding the dynamics of brittle deformation and its correlation with seismic activity is essential for assessing high-risk zones and guiding sustainable urban planning in this region. Our research focuses on evaluating these high-risk dynamic zones by integrating geological surveys, remote sensing, and seismic data analysis. By identifying areas prone to instability, we aim to provide valuable insights for urban planners, engineers, and policymakers to develop safer infrastructure, implement risk mitigation measures, and enhance disaster preparedness in northeastern Kerman.

II. Geology of Studied Location

Iran is situated at the convergence zone between the Arabian Plate, the Eurasian Plate, and the Indian Plate, making it one of the most tectonically active regions in the world (Aghanabati, 2012). This complex interaction has resulted in a diverse range of structural and geological features, including major fault systems, fold-thrust belts, and active seismic zones (Stern et al., 2021). The ongoing collision between the Arabian and Eurasian plates has led to intense crustal deformation, forming key tectonic provinces such as the Zagros Fold and Thrust Belt, the Alborz Mountains, and the Central Iran Plateau (Mirzaei et al., 1998). This tectonic activity is responsible for frequent earthquakes and significant landscape changes over geological timescales (Clapp, 1940). The major fault systems in Iran play a crucial role in accommodating crustal deformation (Aghanabati, 2012). Some of the most prominent ones include the Main Zagros Fault, the Doruneh Fault, the Nayband Fault, and the North Tabriz Fault, all of which contribute to strike-slip and thrust faulting mechanisms (Stöcklin, 1968). The Zagros-Makran Transfer Zone (ZMTZ) marks the transition from the collision-driven tectonics of the Zagros Belt to the subduction-dominated regime of the Makran Trench (Stern et al., 2021). Additionally, the Central Iran Microcontinent, which is bordered by ophiolitic suture zones and strike-slip faults, exhibits a complex interplay of extensional and compressional tectonics, influencing seismic activity in the region (Aghanabati, 2012; Amirihanza et al., 2018).

Iran's tectonic setting has significant implications for geotechnical engineering, earthquake hazard assessment, and natural resource exploration (Stöcklin, 1968; Ebrahimi et al., 2021). The Zagros Belt is rich in hydrocarbons, while the Central Iran region contains numerous mineral deposits formed by tectonically controlled magmatic and hydrothermal processes (Walker & Jackson, 2004). Seismic hazards remain a major concern, with historical earthquakes causing widespread destruction in cities like Tabas, Bam, and Manjil-Rudbar. Understanding the tectonic framework of Iran is essential for infrastructure development, disaster risk reduction, and sustainable resource management in this geologically dynamic region (Camp & Griffis, 1982). Figure 1 presents a simplified tectonic map of Iran overlaid on a shaded-relief image from the Shuttle Radar Topography Mission (SRTM). This map illustrates the major tectonic domains and the primary strike-slip fault systems that accommodate the Arabia-Eurasia convergence (Tadayon et al., 2017). The tectonic framework of Iran is shaped by the ongoing collision between the Arabian and Eurasian plates, leading to a highly complex system of faults and structural zones (Madanipour et al., 2017). The tectonic framework includes major fault systems and tectonic zones, which play a crucial role in accommodating regional deformation (Berra et al., 2017). The inset map provides GPS velocity vectors (black arrows), illustrating the relative motion of Iran with respect to stable Eurasia, based on data from Walpersdorf et al. (2014). The studied region is located in central Iran zone.

Central Iran is a structurally complex region located between the Zagros Fold and Thrust Belt to the southwest and the Alborz Mountains to the north (Aghanabati, 2012). It is characterized by a mosaic of microcontinents, bounded by major strike-slip faults and suture zones that reflect its long tectonic evolution (Stöcklin, 1968). This region has experienced multiple phases of compression, extension, and strike-slip deformation, primarily due to the ongoing collision between the Arabian and Eurasian plates (Stern et al., 2021). The Central Iran Microcontinent is bordered by key fault systems, including the Doruneh Fault, the Nayband Fault, and the Kashmar-Kerman Tectonic Zone (KKTZ), which accommodate significant crustal deformation. The region also features ophiolitic remnants, marking the closure of ancient oceanic basins (Tadayon et al., 2017). The structural configuration of Central Iran, as illustrated in Figure 2, reveals distinct tectonic subdomains, including the Lut Block, Tabas Block, and Yazd Block, which are separated by major fault systems (Aghanabati, 2012). These blocks have been subject to differential uplift and subsidence, leading to varied topography and seismic activity (Berberian, 1981). The region is seismically active, with historical earthquakes indicating ongoing crustal adjustment (Zanchi et al., 2006). Additionally, Central Iran hosts extensive magmatic and mineralized zones, making it a key area for geological and economic studies (Stern et al., 2021). The tectonic evolution of this region continues to be a focus of research, as it plays a crucial role in understanding the broader Arabia-Eurasia collision system and its implications for earthquake hazards and resource exploration (Aghanabati, 2012).

The Kerman region is one of the most geologically diverse and fascinating areas in Iran, characterized by a wide range of geological and tectonic formations (Aghanabati, 2012). This region encompasses multiple tectonic zones, each with distinct structural and lithological features (Ameri et al., 2022). Moving from the northernmost parts of the region towards the south, the complexity of these formations becomes more evident (Walker et al., 2010). A key structural unit in this region is the Central Iran Microcontinent, which forms a significant part of Central Iran (Aghanabati, 2012). This microcontinent is bounded by several major geological features, including the Sistan Ophiolitic Suture Zone, the Naien Ophiolitic Belt, the Baft Ophiolite, the Doruneh Fault, and the Kashmar-Sabzevar Ophiolites (Stöcklin, 1968).

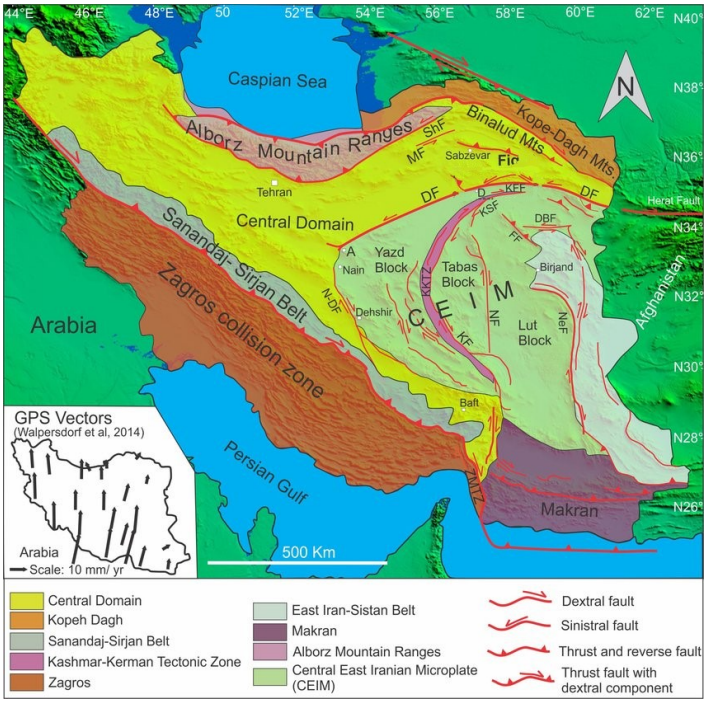

Fig. 1 Simplified tectonic map of Iran (Tadayon et al., 2017)

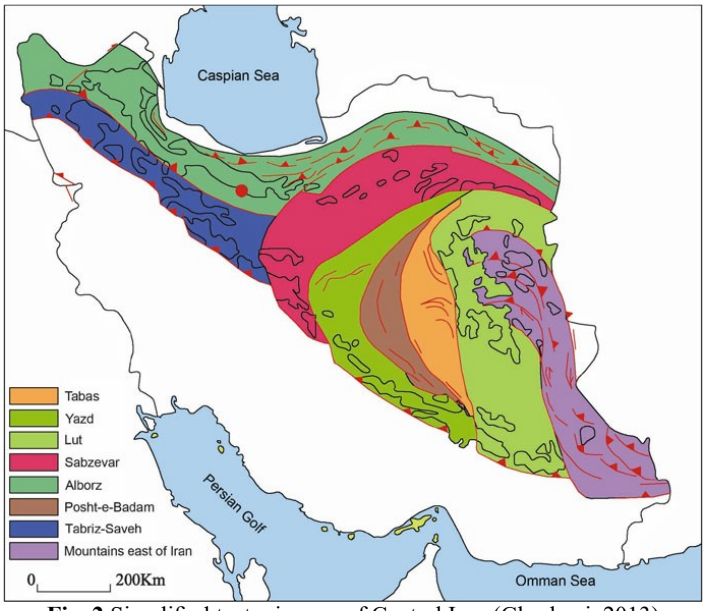

Fig. 2 Simplified tectonic map of Central Iran (Ghorbani, 2013)

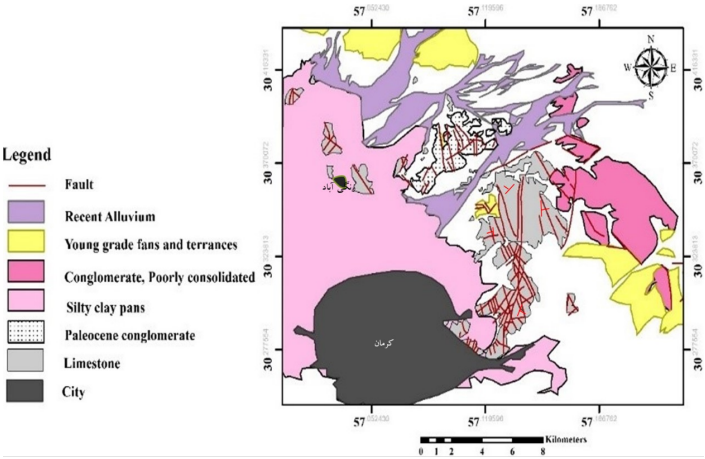

Fig. 3 Geological map of Northeastern Kerman (Geological Survey of Iran, 2010)

It is further segmented by large-scale right-lateral strike-slip faults, which display a characteristic westward curvature. Based on these structural and geological characteristics, the Central Iran Microcontinent can be divided into several distinct tectonic units: the Lut Block, the Shotori Uplift, the Tabas Depression, the Kalmard Uplift, the Posht-e-Badam Block, the Biyaz-Bardsir Graben, and the Yazd Block. Each of these units has undergone unique geological processes, contributing to the rich tectonic and mineralogical complexity of the region. Their interactions have played a crucial role in shaping the geological landscape of Kerman, making it an essential area for further geological, geotechnical, and mineral exploration studies. Figure 3 is provided the geological map of the studied area. The Cretaceous limestones around the city of Kerman have extensive outcrops. The lithological sequence of these outcrops includes marly sandstone limestones, marly limestones, bioclastic limestones, detrital-bioclastic limestones, and micritic limestones along with marl. In the study area, Aliabad Mountain is visible, as shown in Figure 3. According to the geological map of Kerman (Geological Survey of Iran, 2010), the Cretaceous sequence in this region outcrops in the plunging anticline structure (Aghanabati, 2012). The northwestern parts of the Cretaceous outcrop in this area are covered by the Kerman conglomerate, which is a result of tectonic displacement (Ghorbani, 2013). The geological formation of this area is characterized by complex tectonic features and various rock types. The limestones in the region are indicative of shallow marine deposits, while the Kerman conglomerate suggests more dynamic conditions during the Cenozoic (Aghanabati, 2012). The transition from limestones to conglomerates represents a significant shift in depositional environments, influenced by tectonic forces and regional uplift (Ghorbani, 2013). Additionally, an aerial map of the region is provided in Figure 4, which offers a detailed view of the landscape and geological formations.

In accordance with the geological map, the cretaceous formations in the Kerman area are divided into Early and Late Cretaceous periods. The Late Cretaceous is more prevalent, while the Early Cretaceous is relatively thin. The Late Cretaceous is further divided into two groups. One outcrop, located 15 km northeast of Deh Mohammad Shah, shows a sequence of conglomerates and red sandstone-shales overlying the K_1^{mg} unit. Above this, marls, marl-limestones, and limestones, attributed to the Lower Senonian, are found. This sequence is followed by a 2-3m, thick conglomerate, succeeded by dark grey to black reef-rudist-bearing limestone. The majority of Saidi Mountain is composed of this unit.

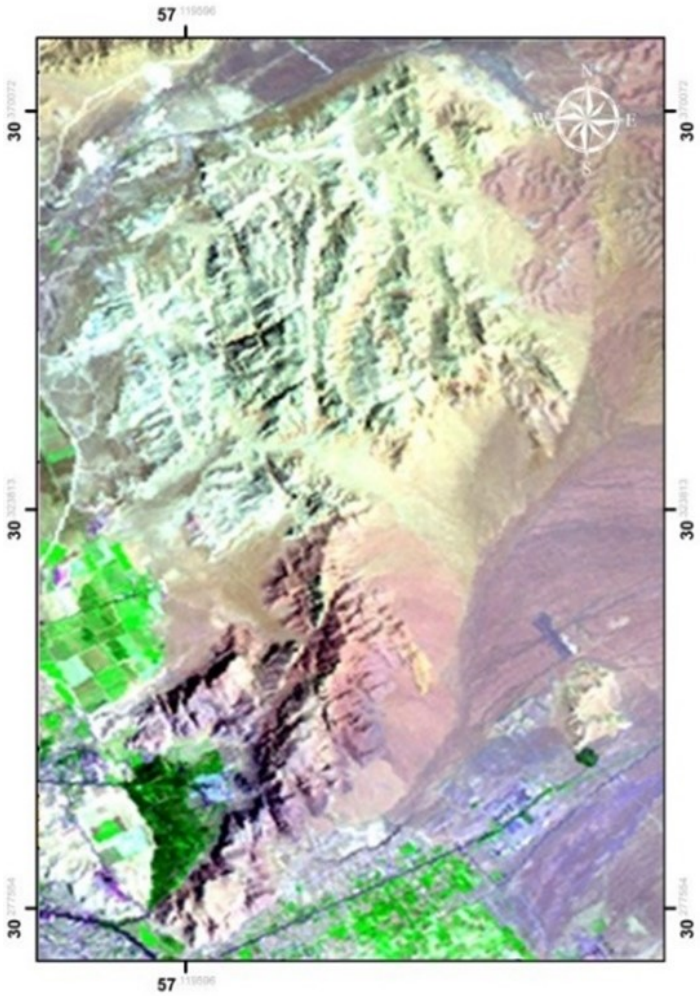

Fig. 4 Satellite image of the study area (Landsat TM data)

The Quaternary sedimentary unit, Q^{pic}, covers large areas in the northern and eastern parts of the region. It consists of unconsolidated conglomerates, mainly horizontal, except in fault zones where they are cemented. The area also contains sand dunes and windblown sands in the northeast. Older alluvial fans (Q_1^{t1}, Q_1^{t2}) are cut by younger alluvial fans and floodplains (Q_2^{t1}, Q_2^{t2}), with younger deposits being associated with riverbeds, wind-blown sediments, and debris. Metamorphic rocks in the area, such as skarns and marbles, form due to the intrusion of basic dikes into Upper Cretaceous limestones, with outcrops seen in the Jangal-e-Ghaem region. Igneous rocks, including monzonitic and diabase dikes, are found in areas like Kuh-e-Saheb-al-Zaman and Saidi stone quarries, exhibiting a porphyritic texture. These dikes contain clinopyroxenes that often alter into biotite, and the groundmass is made of plagioclase and alkali feldspar. Some dikes undergo intense alteration, converting minerals into calcite, chlorite, and albite.

III. High-Risk Dynamic Zones Analysis

The in-situ stress field plays a crucial role in shaping the geological and geomorphological features of northeastern Kerman. The region is characterized by a complex network of faults, fractures, and brittle deformation structures, which are primarily controlled by regional tectonics (Bell, 2007). These stress-induced discontinuities have resulted in various high-risk dynamic zones that are susceptible to instability, posing significant challenges for infrastructure development and urban expansion (Hencher, 2013). Figure 5 illustrates an example of in-situ stress field in a large-area (Twiss & Moores, 2006). The intricate fault systems in northeastern Kerman, including major strike-slip and thrust faults, have led to diverse morphological landforms such as fault scarps, uplifted blocks, and subsided basins. These features are strongly influenced by the orientation and intensity of the regional stress regime. The continuous tectonic activity has not only shaped the landscape but also contributed to geotechnical hazards, including slope failures, differential settlements, and seismic-induced deformations. The dependency of morphological structures on the prevailing stress field is evident through the spatial distribution of brittle deformation zones. Northeastern Kerman lies at the convergence of several active fault zones, where stress accumulation leads to localized shearing, tension fractures, and block rotations. The tectonic control over these deformations dictates the stability of slopes, foundation conditions, and subsurface integrity, making it crucial to analyze these factors for engineering applications. Understanding the spatial distribution of high-risk dynamic zones is essential for geotechnical and urban planning projects. This knowledge is particularly beneficial in determining the safest locations for infrastructure development, reducing the risks associated with seismic activity and ground instability. In geotechnical design, recognizing the influence of brittle deformation on soil and rock mechanics helps in optimizing foundation systems and excavation techniques. For instance, areas affected by fault-induced fracturing may require specialized reinforcement measures, such as deep foundations, retaining structures, and ground improvement techniques, to mitigate settlement and instability issues.

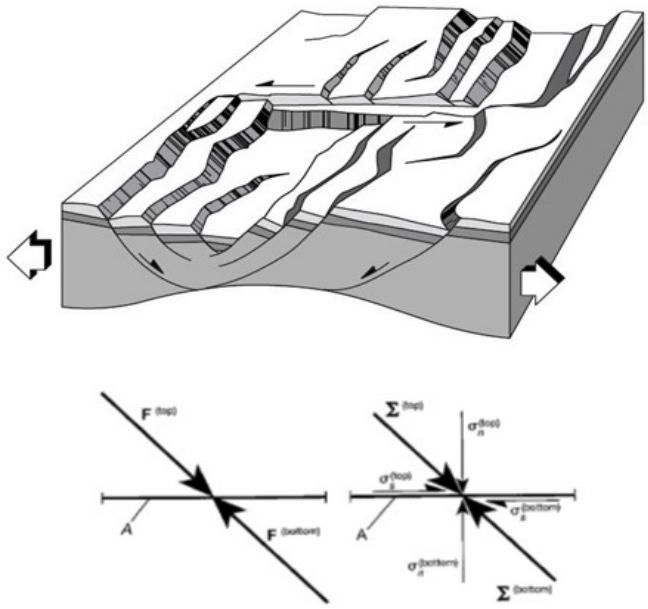

Fig. 5 A simplified example for in-situ stress field (Twiss & Moores, 2006)

The presence of high-risk dynamic zones also has implications for hydrology and groundwater flow patterns. Fault zones often act as conduits or barriers to subsurface water movement, influencing the distribution of aquifers and potential flooding risks (Twiss & Moores, 2006). In northeastern Kerman, where water scarcity is a concern, understanding these structural controls is vital for sustainable water resource management and land-use planning. From an urban development perspective, integrating tectonic hazard assessments into zoning regulations can significantly enhance disaster resilience. By mapping out high-risk deformation zones, authorities can establish buffer zones around active faults, enforce stricter building codes, and implement early warning systems to protect communities from potential geohazards. The role of geospatial technologies, such as remote sensing and GIS-based modeling, is invaluable in analyzing high-risk dynamic zones. By combining satellite imagery with field-based geological investigations, researchers can accurately delineate fault-controlled deformations and predict areas of future instability. This approach enables proactive risk management strategies that can prevent catastrophic failures. As northeastern Kerman continues to experience tectonic activity, continuous monitoring of stress-related deformation is necessary to refine geotechnical models and improve hazard mitigation strategies. The integration of geophysical surveys, stress-strain analysis, and seismic monitoring networks will provide a more comprehensive understanding of the evolving stress regime in the region. The study area in this research is classified as an extensional zone. According to Shahabpour (2005), this region has developed within the back-arc setting resulting from the subduction of the Neotethys Ocean beneath the Iranian Plate. The presence of normal faults and dykes within the area serves as strong evidence of this extensional regime. These geological structures indicate a history of tensional forces that have significantly influenced the region's geodynamic evolution (Mirzababaei & Shahabpour, 2014).

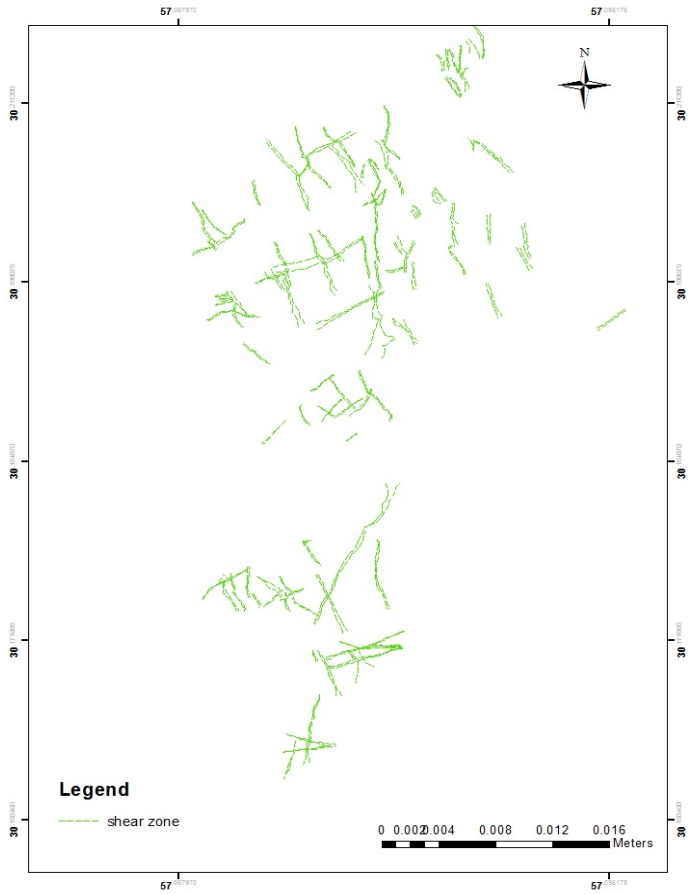

Fig. 6 Map of the shear zones of the study area

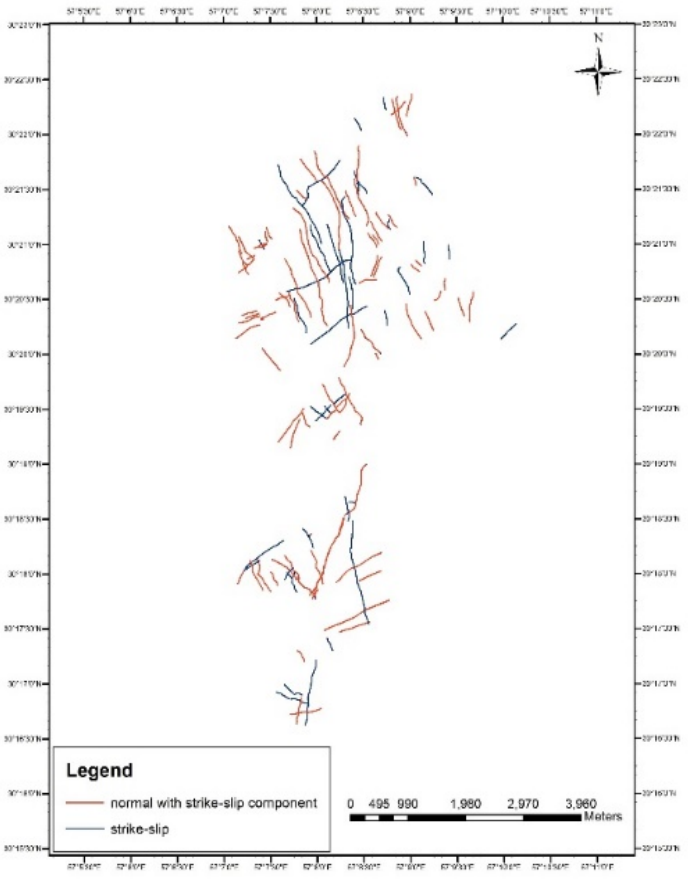

Fig. 7 Map of the studied region's main faults

Widespread shear zones are observed throughout the study area (Figure 6), which have formed due to a combination of tensile and shear fractures, commonly referred to as hybrid fractures. These hybrid fractures are characterized by oblique displacement along the fracture surface, occurring under conditions where the minimum principal stress (σ_3) is less than the normal stress (σ_n) but still within a range that allows tensile failure to dominate ($\sigma_3 < \sigma_n < 0$). This stress state promotes the formation of dilation faults, which accommodate extensional strain and facilitate the intrusion of magma, leading to the development of dykes. The presence of extensional structures such as normal faults, dykes, and hybrid fractures suggests that the study area has undergone significant tectonic stretching. This extensional regime is a direct result of the regional tectonic forces acting in the aftermath of the Neotethys subduction. The movement along these structures not only contributes to the overall deformation pattern of the region but also influences the mechanical properties of the rock mass, affecting its stability and behavior under stress conditions (Figure 7). In addition to normal faulting, the extensive shear fractures in the region highlight the progressive deformation that has taken place over geological time. These shear structures are commonly associated with zones of high strain concentration, where the combined effects of compressive and extensional stresses lead to complex deformation patterns. The hybrid nature of these fractures suggests a transitional stress regime where both brittle and ductile deformation mechanisms interact, further complicating the region's structural evolution.

Understanding the distribution and orientation of these tectonic features is crucial for several applications, including geotechnical engineering, resource exploration, and seismic hazard assessment. The formation of dilation faults and hybrid fractures can create weak zones within the rock mass, making certain areas more susceptible to landslides, rockfalls, and ground subsidence. Moreover, these structures can act as fluid pathways, influencing groundwater movement and the formation of mineral deposits in the region. The study of these high-risk dynamic zones is particularly important for infrastructure development, as identifying regions with intense extensional deformation can help engineers design safer foundations and more resilient structures. Furthermore, the interaction of normal faulting and shear fracturing plays a significant role in the seismic activity of the region, making it essential to incorporate tectonic analyses into urban planning and disaster management strategies.

IV. Kinematic Stress Analysis For Northeastern Kerman

The study area, covering approximately 50 km^2, is in the northeastern part of Kerman Province. This region features extensive outcrops of Cretaceous-aged limestones with a diverse lithological sequence. The exposed rock units primarily consist of sandy marl limestones, marl limestones, bioclastic limestones, detrital-bioclastic limestones, micritic limestones, and marls. One

of the most prominent structural features in these limestones is the presence of fault systems exhibiting both normal and strike-slip kinematics, which have played a key role in shaping the region's geological framework. Detailed structural analyses indicate that strike-slip faults are younger than normal faults in this region. The average dip of faulted layers provides further evidence of this chronological relationship, with strike-slip faults showing an average dip of 69 degrees, whereas normal faults exhibit a steeper dip of 76.5 degrees. Among the surveyed faults, 14 normal faults with distinct slickenlines and 26 well-defined strike-slip faults were selected for paleostress analysis. These faults were chosen based on their high-quality slip indicators and optimal mechanical conditions, ensuring reliable results (Figures 8 and 9). To minimize uncertainties in fault kinematics, only faults with clear slip indicators, such as fault steps, striations, and associated secondary fractures, were incorporated into the final stress analysis. Paleostress analysis serves as a fundamental tool for understanding the structural evolution of tectonically active regions, particularly in areas affected by brittle deformation. This method is especially valuable in deciphering complex fault networks, where multiple stress phases have influenced fault activity over time. The primary objective of paleostress analysis is to reconstruct the stress tensor responsible for fault slip, a process commonly referred to as the inverse problem.

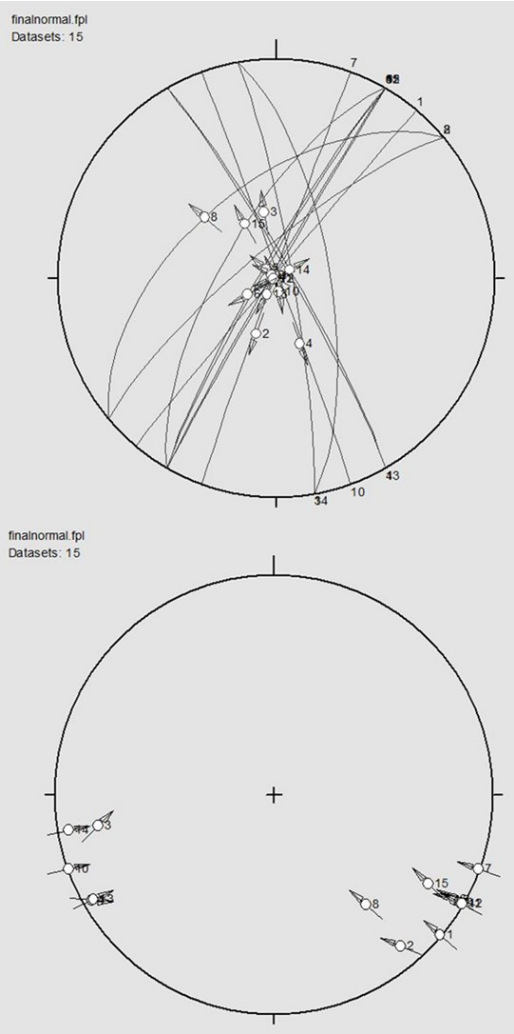

Fig. 8 Stereographic graph of faults in the study area

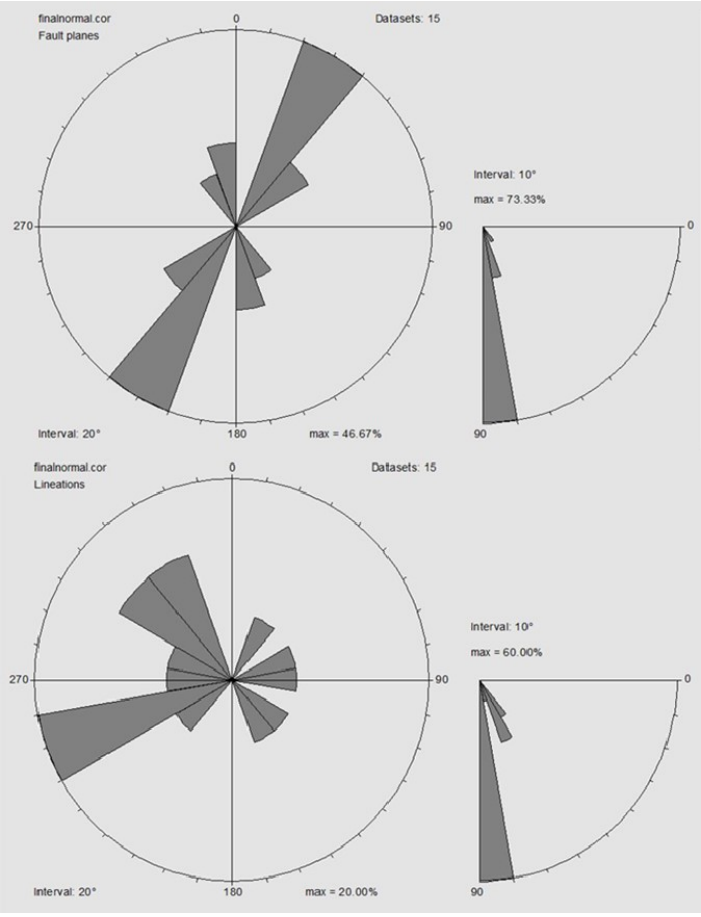

Fig. 9 Rose diagrams of shear zones with faults in the study area

To determine the orientation of slip vectors, two critical factors are considered: the orientation of the principal stress axes and the geometric shape of the stress ellipsoid. According to Anderson's theory of faulting, the relative positioning of the three principal stress axes (σ_1, σ_2, and σ_3) dictates the faulting regime. If σ_1 (maximum principal stress) is vertical, normal faulting occurs; if σ_2 (intermediate stress) is vertical, strike-slip faulting occurs; and if σ_3 (minimum principal stress) is vertical, reverse faulting dominates (Twiss & Moores, 2006). Several researchers argue that one of the principal stress axes must always be vertical during fault activity. Based on this assumption, in the study area, σ_1 is considered vertical for normal faults, while σ_2 is assumed to be vertical for strike-slip faults. To gain a more comprehensive understanding of the regional stress field, all fault-slip data were plotted on stereonets, ensuring that for normal faults, σ_1 is placed at the stereonet center, while for strike-slip faults, σ_2 is positioned at the center.

The orientation and elliptical shape of the regional stress field exert significant control over the type, spatial distribution, and slip direction of faults in the study area. As proposed by Angelier (1994), stress field geometry dictates fault development and kinematics, influencing how faults propagate and accommodate strain. The process of determining the regional stress field from fault-slip data is known as stress inversion, which helps reconstruct the tectonic history of an area. The findings from this study contribute to a deeper understanding of the tectonic forces shaping northeastern Kerman.

One of the key factors influencing paleostress analysis is the friction angle (ϕ) of the rock mass during fault system activity where main value in geotechnical designs. In this study, the R% graph method and the fault plane analysis method were employed to determine this angle. The following sections provide a detailed explanation of these methods. In R% approach, selected friction angles are plotted on the x-axis, while R% values are plotted on the y-axis. By analyzing the normal faults in the study area, two critical angles were obtained: 82 degrees at the maximum point and 45 degrees at the minimum point of the graph. According to Marin et al. (2004), the maximum point of the R% graph represents the internal friction angle of the rock mass at the time of fault system activity. Based on this, the 45-degree angle was selected as the internal friction angle for the rock mass in the study area (Figure 10a). Similarly, for strike-slip faults, the R% method yielded 84 degrees at the maximum point and 45 degrees at the minimum point. As a result, the 45-degree angle was adopted as the internal friction angle of the rock mass during faulting, confirming its consistency across different fault types (Figure 10b). These findings provide critical insights into fault mechanics and stress conditions at the time of fault activation, aiding in the broader understanding of tectonic processes and geomechanical properties of the study area.

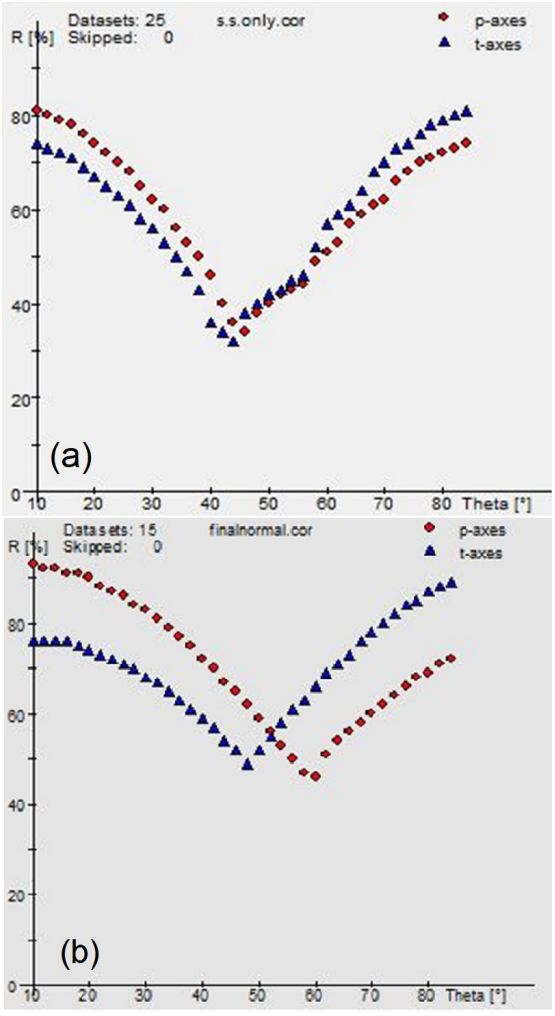

Fig. 10 Variations in the friction angle with R%: (a) normal, (b) strike-slip faults

Understanding the orientation of compression (P) and tension (T) axes is essential for reconstructing the paleostress field and analyzing the kinematic behavior of faults. In the northeastern Kerman region, where both normal and strike-slip faults are present, identifying these axes provides valuable insights into the tectonic forces governing the region. The results of this analysis are illustrated in Figure 11, which presents stereographic projections of the P and T axes for normal and strike-slip faulting. The P-axis represents the direction of σ_1, whereas the T-axis corresponds to the σ_3. These axes are determined using fault slip analysis, where the orientation of fault planes and the direction of slip are used to derive the stress tensor responsible for faulting. By mapping these axes, the prevailing stress regimes in the study area can be better understood.

The first step in this analysis involved collecting fault slip data from extensive field surveys. Measurements were taken from fault planes, slickenlines, and fault-related structures, with a focus on determining shear stress orientations. The data were then plotted on a lower hemisphere equal-area stereonet, allowing for the identification of the principal stress directions. For normal faults, the T-axis is typically oriented vertically, corresponding to the direction of σ_3. The P-axis, on the other hand, lies within the horizontal plane, perpendicular to the extension direction. The stereographic projections presented in Figure 11a confirm a consistent extensional trend across the region, indicating that normal faulting is controlled by crustal extension forces. In contrast, strike-slip faults exhibit a different stress distribution. For these faults, the P-axis lies in the horizontal plane, aligned with the σ_1, while the T-axis is also horizontal, aligned with the σ_3. This pattern suggests a shear-dominated stress regime, which is clearly reflected in the distribution of strike-slip fault P and T axes in Figure 11b.

The orientation of these axes has significant tectonic implications. The observed normal faults suggest that the region has experienced active crustal extension, possibly linked to post-collisional tectonic relaxation. Meanwhile, the presence of strike-slip faults indicates a secondary stress regime, associated with lateral displacement along major fault zones. This combination of extensional and shear stress fields highlights the complex tectonic evolution of the region. A comparison of the derived P and T axes with regional stress models reveals a strong correlation between the northeastern Kerman stress field and the broader tectonic framework of central Iran. The results suggest that the region is currently influenced by a NW-SE extensional regime, superimposed by localized transpressional forces. These findings align with previous studies, reinforcing the idea that the area is undergoing progressive deformation due to ongoing tectonic activity. The precise determination of P and T axes is crucial for understanding fault mechanics and assessing the seismic potential of the region. The ability to reconstruct the paleostress field allows for better predictions of fault reactivation, which is vital for urban planning and geotechnical projects in the area. So, the analysis of compression and tension axes in the northeastern Kerman region provides essential data on the regional stress regime and fault kinematics. The results, illustrated in Figure 12, confirm the coexistence of normal and strike-slip faulting, with distinct stress orientations governing each fault type.

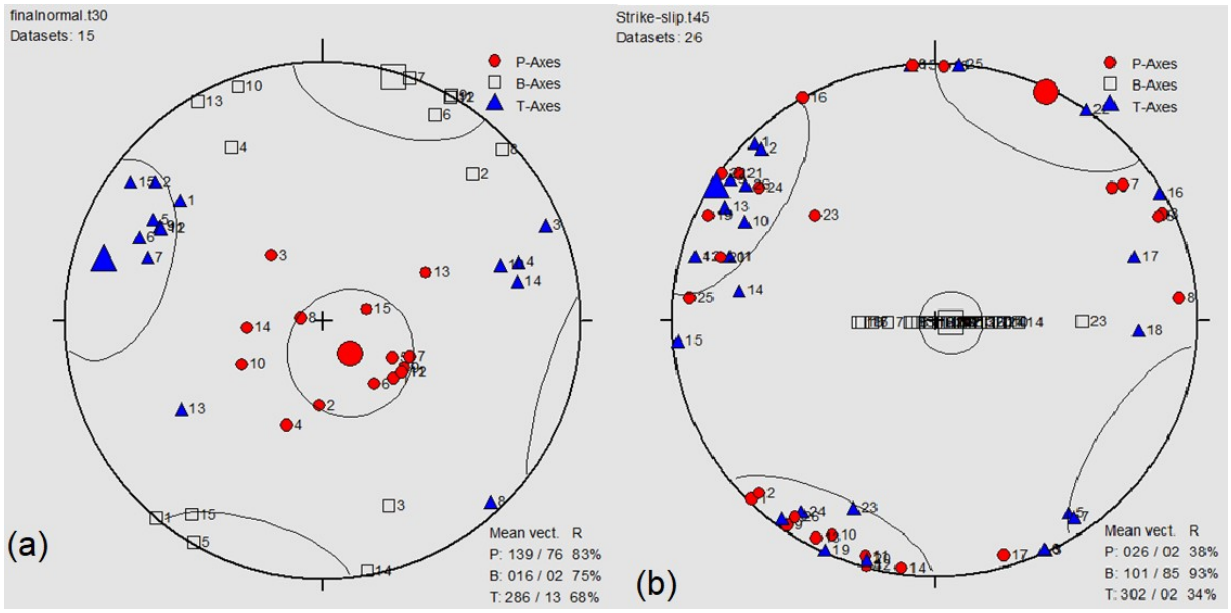

Fig. 11 Stereographic graph for P and T: (a) normal, (b) strike-slip faults

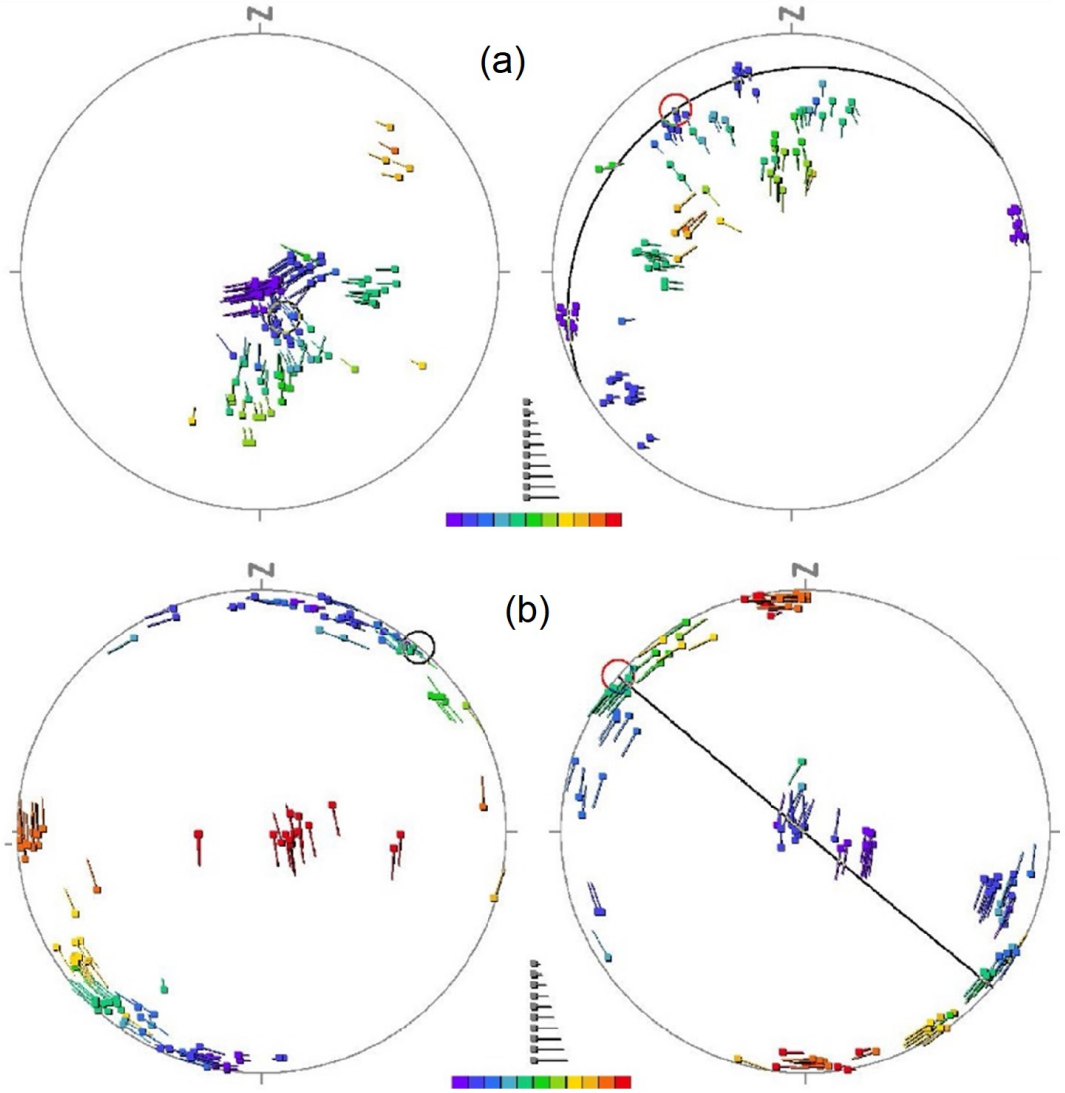

Fig. 12 Left stereogram shows σ_1 position, and right stereogram shows σ_3 position (circular markers). The color spectrum represents stress field variations, from prolate (purple) to oblate (red): (a) normal, (b) strike-slip faults

All faults that share the same components in the four-dimensional space of the reduced stress tensor can be considered as part of a single stress phase. In other words, when the principal stress axes and the stress field shape form a clustered distribution in the four-dimensional tensor space, they are regarded as belonging to a distinct phase of stress. Fault sets observed in the field often experience multiple stress phases over time. This results in heterogeneous datasets, necessitating a method for differentiating stress phases. If a collected fault dataset consists of N faults and needs to be divided into K subsets, the number of possible solutions follows the combinatorial equation (Yamaji, 2000):

$$NCK = \frac{N!}{K!(N-K)!} \quad (1)$$

Initially, fault-slip data are analyzed using a selected stress inversion method to determine the principal stress axes and stress field shape. Data points that exhibit a clustered pattern are identified as a subgroup representing a distinct stress phase and are separated from the remaining dataset. To simultaneously consider both stress axis orientation and field shape, the solutions are visualized as bar symbols on two stereonets, using the visible Newtonian color spectrum (Yamaji, 2000). In this visualization method, the clustered data points on the left stereonet indicate the position of σ_1 (maximum principal stress axis). Simultaneously, a great circle appears on the right stereonet, where symbols matching the color of the first stereonet concentrate to indicate the location of σ_3.

Since the stress shape ratio (Φ) varies between 0 and 1, this range is divided into 11 equal intervals, each representing a 0.1 increment in Φ. Different colors correspond to different stress field shapes:

- Purple represents $\Phi = 0$, corresponding to a prolate (cigar-shaped) ellipsoid.
- Red represents $\Phi = 1$, corresponding to an oblate (disk-shaped) ellipsoid.

In the study area, this method was applied to determine the orientation of principal stress axes and the shape of the stress field. The results, illustrated in Figure 12, provide a detailed representation of the stress regime variations in the region. This technique allows for a comprehensive understanding of fault kinematics, aiding in the interpretation of tectonic evolution and geomechanical stability.

In paleostress analysis, the shape of the stress ellipsoid can be determined using the direct inversion method with unscaled Mohr circles. These circles represent the relative normal and shear stresses calculated from the stress tensor for each fault plane, without showing the absolute values of the principal stresses. The distance between the stress axes (σ_1 and σ_3) is arbitrary, but the ratio of stress differences is displayed. The relative positions of Mohr circles are used to calculate shear stress for each fault plane, and these circles represent the equivalent ellipsoid. For this study, Mohr circles were drawn for normal and strike-slip faults, assuming a 45-degree friction angle. For normal faults, the shape factor (R = 0.43) indicates a flat stress ellipsoid, with a second-type ellipsoid shape.

Some data points were located at the intersection of the vertical line passing through σ_2 with the σ_1-σ_3 plane, suggesting conjugate shear planes. For strike-slip faults, the shape factor (R = 0.45) also indicated a flat, second-type ellipsoid. Many data points intersected at the same location, indicating conjugate shear planes. Using the lineation and Warren methods, the stress field shape was found to be prolate in both normal and strike-slip faulting periods. The analysis of the study area revealed that normal faulting showed a near-vertical maximum compressive stress and a horizontal minimum compressive stress at NW orientation. In strike-slip faulting, the maximum compressive stress was at SSE orientation, and the smallest compressive stress was at NW orientation, with both having a dip of zero. The results confirmed that the stress field shape is prolate, and the region has experienced multiple stress phases.

V. Conclusion

Based on the findings of this study, it can be concluded that the paleostress analysis in the northeastern Kerman region reveals complex tectonic interactions, dominated by both normal and strike-slip faulting. The region's structural features, including fault systems and the resulting morphologies, are strongly influenced by the regional stress field, which is primarily controlled by tectonic forces. The determination of stress tensor components and the use of methods such as Mohr circles and inversion techniques have provided valuable insights into the stress field and faulting mechanisms in this area. The stress ellipsoid shapes observed for both normal and strike-slip faults are of the second type, indicating a dominant prolate stress regime. The analysis of fault orientations and stress directions shows that normal faults exhibit a near-vertical maximum compressive stress and horizontal minimum compressive stress in the northwest direction. In contrast, strike-slip faults demonstrate a maximum compressive stress oriented SSE, with a minimal compressive stress also aligned in the northwest direction. These findings suggest a complex history of stress evolution, with the region having undergone multiple stress phases over time. Furthermore, the study emphasizes the importance of understanding the relationship between fault kinematics and the regional stress field for geotechnical and urban development applications. The identification of shear zones, fault slip behaviors, and stress orientations provides critical data for future hazard assessments and infrastructure planning in this seismically active region. Overall, the study contributes to a deeper understanding of the tectonic processes in northeastern Kerman and their implications for regional structural development and seismic risk management.

Acknowledgment

We would like to express our sincere gratitude to the editorial team for their valuable feedback and guidance throughout the review process. Additionally, we extend our thanks to the reviewers for their meticulous attention to detail and constructive suggestions that greatly improved the quality of this manuscript. Your contributions have been instrumental in shaping this work.

Authors' contributions

Anis Akbarzadeh and Shahbaz Radfar conducted the main data analysis, contributed to the data collection, preprocessing, and interpretation, and were responsible for drafting the initial manuscript. Shahram Shafiei Bafti assisted in

the development of the methodology and performed validation checks, provided supervision, conceptual guidance, and critical revision of the manuscript. All authors read and approved the final manuscript.

CONFLICT OF INTEREST

The authors have not disclosed any competing interests.

OPEN ACCESS

This article is distributed under the terms of the *Creative Commons Attribution 4.0 International License*, which allows use, sharing, adaptation, distribution, and reproduction in any medium or format, provided appropriate credit is given to the original author(s) and the source. A link to the Creative Commons license must also be provided, and any modifications should be clearly indicated. Unless otherwise noted in a credit line, images or third-party materials included in this article are covered under the article's Creative Commons license. For material not included in the license or where statutory regulations do not apply, permission must be obtained directly from the copyright holder. To view the full license, visit http://creativecommons.org/licenses/by/4.0/.

Publisher's Note: This journal remains neutral with regard to jurisdictional claims in published maps, data, and institutional affiliations.

REFERENCES

Aghanabati A. (2012). *Geology of Iran*. Geological Survey of Iran press, Tehran, Iran.

Ahmad R.A., Singh R.P., Adris A. (2017). Seismic hazard assessment of Syria using seismicity, DEM, slope, active faults and GIS. *Remote Sensing Applications: Society and Environment*, 6, 59-70. https://doi.org/10.1016/j.rsase.2017.04.003.

Ahmadi H., Pekkan E. (2021). Fault-based geological lineaments extraction using remote sensing and GIS—a review. *Geosciences*, 11(5), 183. https://doi.org/10.3390/geosciences11050183.

Ameri S., Solgi A., Sorbi A., Farrokhnia A. (2022). Identification of faults with seismic hazard potential based on morphotectonic analysis, Kerman city (Southeastern Iran). *Earth Sciences Research Journal*, 26(1), 23-38. https://doi.org/10.15446/esrj.v26n1.83186 .

Amirihanza H., Shafieibafti S., Derakhshani R., Khojastehfar S. (2018). Controls on Cu mineralization in central part of the Kerman porphyry copper belt, SE Iran: constraints from structural and spatial pattern analysis. *Journal of Structural Geology*, 116, 159-177. https://doi.org/10.1016/j.jsg.2018.08.010.

Angelier, J. (1994). Fault slip analysis and palaeostress reconstruction. *Continental Deformation*, 1994, 53-100.

Atkinson B.K. (2015). *Fracture mechanics of rock*. Elsevier, Amsterdam, The Netherlands.

Avar B.B., Hudyma N.W. (2019). Earthquake surface rupture: a brief survey on interdisciplinary research and practice from geology to geotechnical engineering. *Rock Mechanics and Rock Engineering*, 52(12), 5259-5281. https://doi.org/10.1007/s00603-019-02006-0.

Barreca G., Bonforte A., Neri M. (2013). A pilot GIS database of active faults of Mt. Etna (Sicily): A tool for integrated hazard evaluation. *Journal of Volcanology and Geothermal Research*, 251, 170-186. https://doi.org/10.1016/j.jvolgeores.2012.08.013.

Bell F.G. (2007). *Engineering geology*. Elsevier, Amsterdam, The Netherlands.

Berberian M. (1981). Active faulting and tectonics of Iran. *Zagros Hindu Kush Himalaya Geodynamic Evolution*, 3, 33-69.

Berra F., Zanchi A., Angiolini L., Vachard D., Vezzoli G., Zanchetta S., Kouhpeyma M. (2017). The upper Palaeozoic Godar-e-Siah Complex of Jandaq: evidence and significance of a North Palaeotethyan succession in Central Iran. *Journal of Asian Earth Sciences*, 138, 272-290. https://doi.org/10.1016/j.jseaes.2017.02.006.

Bird J.F., Bommer J.J. (2004). Earthquake losses due to ground failure. *Engineering Geology*, 75(2), 147-179.

Blyth F.G.H., De Freitas M. (2017). *A geology for engineers*. CRC Press, Boca Raton, Florida, USA.

Brideau M.A., Yan M., Stead D. (2009). The role of tectonic damage and brittle rock fracture in the development of large rock slope failures. *Geomorphology*, 103(1), 30-49. https://doi.org/10.1016/j.geomorph.2008.04.010.

Camp V.E., Griffis R.J. (1982). Character, genesis and tectonic setting of igneous rocks in the Sistan suture zone, eastern Iran. *Lithos*, 15(3), 221-239.

Chigira M. (1992). Long-term gravitational deformation of rocks by mass rock creep. *Engineering Geology*, 32(3), 157-184.

Clapp F.G. (1940). Geology of eastern Iran. *Bulletin of the Geological Society of America*, 51(1), 1-102.

Deligiannakis G., Papanikolaou I.D., Roberts G. (2018). Fault specific GIS based seismic hazard maps for the Attica region, Greece. *Geomorphology*, 306, 264-282. https://doi.org/10.1016/j.geomorph.2016.12.005.

Ebrahimi Y., Shafieibafti S., Derakhshani R., Esmaeilian S. (2021). Slip partitioning and inclined transpression in the Bazargan fold and thrust belt, Central Iran Microcontinent, Kerman area, SE Iran. *Journal of Structural Geology*, 148, 104352.

Fasching F., Vanek R. (2011). Engineering geological characterisation of fault rocks and fault zones/Ingenieurgeologische Charakterisierung von Störungsgesteinen und Störungszonen. *Geomechanics and Tunnelling*, 4(3), 181-194. https://doi.org/10.1002/geot.201100013.

Geological Survey of Iran, GSI (2010). *Geological map and information sheets for northeastern of Kerman in 1:100,000 and 1:250,000 scale*. Maps unit, Geological Survey and Mineral Exploration of Iran press, Tehran, Iran.

Ghorbani, M. (2013). *The economic geology of Iran: Mineral deposits and natural resources*. Springer, Heidelberg, Germany.

Harris R.A. (2017). Large earthquakes and creeping faults. *Reviews of Geophysics*, 55(1), 169-198. https://doi.org/10.1002/2016RG000539.

Hashemi M., Alesheikh A.A. (2011). A GIS-based earthquake damage assessment and settlement methodology. *Soil Dynamics and Earthquake Engineering*, 31(11), 1607-1617. https://doi.org/10.1016/j.soildyn.2011.07.003.

Hencher S. (2013). Practical engineering geology. *Environmental & Engineering Geoscience*, 19(2), 201-203. https://doi.org/10.2113/gseegeosci.19.2.201.

Hulbert C., Rouet-Leduc B., Johnson P.A., Ren C.X., Rivière J., Bolton D.C., Marone C. (2019). Similarity of fast and slow earthquakes illuminated by machine learning. *Nature Geoscience*, 12(1), 69-74. https://doi.org/10.1038/s41561-018-0272-8.

Karimzadeh S., Miyajima M., Hassanzadeh R., Amiraslanzadeh R., Kamel B. (2014). A GIS-based seismic hazard, building vulnerability and human loss assessment for the earthquake scenario in Tabriz. *Soil Dynamics and Earthquake Engineering*, 66, 263-280. https://doi.org/10.1016/j.soildyn.2014.06.026.

Killick A.M. (2003). Fault rock classification: an aid to structural interpretation in mine and exploration geology. *South African Journal of Geology*, 106(4), 395-402. https://doi.org/10.2113/106.4.395.

Krinitzsky E.L. (2002). How to obtain earthquake ground motions for engineering design. *Engineering Geology*, 65(1), 1-16. https://doi.org/10.1016/S0013-7952(01)00098-9.

Lin M.L., Lin C.H., Li C.H., Liu C.Y., Hung C.H. (2021). 3D modeling of the ground deformation along the fault rupture and its impact on engineering structures: Insights from the 1999 Chi-Chi earthquake, Shigang District, Taiwan. *Engineering Geology*, 281, 105993. https://doi.org/10.1016/j.enggeo.2021.105993.

Lin M.L., Tung C.C. (2004). A GIS-based potential analysis of the landslides induced by the Chi-Chi earthquake. *Engineering Geology*, 71(1-2), 63-77. https://doi.org/10.1016/S0013-7952(03)00126-1.

Liu J.G., Mason P.J., Yu E., Wu M.C., Tang C., Huang R., Liu H. (2012). GIS modelling of earthquake damage zones using satellite remote sensing and DEM data. *Geomorphology*, 139, 518-535. https://doi.org/10.1016/j.geomorph.2011.12.002.

Madanipour S., Ehlers T.A., Yassaghi A., Enkelmann E. (2017). Accelerated middle Miocene exhumation of the Talesh Mountains constrained by U-Th/He thermochronometry: Evidence for the Arabia-Eurasia collision in the NW Iranian Plateau. *Tectonics*, 36(8), 1538-1561. https://doi.org/10.1002/2016TC004291.

Mandl G. (1999). *Faulting in brittle rocks: an introduction to the mechanics of tectonic faults*. Springer Science & Business Media, Heidelberg, Germany.

Marin S., Avouac J.P., Nicolas M., Schlupp A. (2004). A probabilistic approach to seismic hazard in metropolitan France. *Bulletin of the Seismological Society of America*, 94(6), 2137-2163.

Mehrabi A., Pirasteh S., Rashidi A., Pourkhosravani M., Derakhshani R., Liu G., Xiang W. (2021). Incorporating persistent scatterer interferometry and radon anomaly to understand the anar fault mechanism and observing new evidence of intensified activity. *Remote Sensing*, 13(11), 2072. https://doi.org/10.3390/rs13112072.

Mirzababaei G.H., Shahabpour J. (2014). Large-magnitude Ring structures as structural precursors for porphyry Cu deposit formation in Kerman copper belt, Iran. *Journal of Tethys*, 2(4), 375-394.

Mirzaei N., Mengtan G., Yuntai C. (1998). Seismic source regionalization for seismic zoning of Iran: major seismotectonic provinces. *Journal of Earthquake Prediction Research*, 7, 465-495.

Paronuzzi P., Bolla A. (2015). Gravity-induced rock mass damage related to large en masse rockslides: evidence from Vajont. *Geomorphology*, 234, 28-53. https://doi.org/10.1016/j.geomorph.2015.01.008.

Rahman N., Ansary M.A., Islam I. (2015). GIS based mapping of vulnerability to earthquake and fire hazard in Dhaka city, Bangladesh. *International Journal of Disaster Risk Reduction*, 13, 291-300. https://doi.org/10.1016/j.ijdrr.2015.07.003.

Riedmüller G., Brosch F.J., Klima K., Medley E.W. (2001). Engineering geological characterization of brittle faults and classification of fault rocks. *Felsbau*, 19(4), 13-19.

Rodríguez-Peces M.J., García-Mayordomo J., Azañón J.M., Jabaloy A. (2014). GIS application for regional assessment of seismically induced slope failures in the Sierra Nevada Range, South Spain, along the Padul Fault. *Environmental Earth Sciences*, 72, 2423-2435. https://doi.org/10.1007/s12665-014-3151-7.

Rouet-Leduc B., Hulbert C., Lubbers N., Barros K., Humphreys C.J., Johnson P. A. (2017). Machine learning predicts laboratory earthquakes. *Geophysical Research Letters*, 44(18), 9276-9282. https://doi.org/10.1002/2017GL074677.

Scawthorn C., Chen W.F. (2002). *Earthquake Engineering Handbook*. CRC press, Boca Raton, Florida, USA.

Schultz R.A. (1996). Relative scale and the strength and deformability of rock masses. *Journal of Structural Geology*, 18(9), 1139-1149. https://doi.org/10.1016/0191-8141(96)00045-4.

Shahabpour J. (2005). Tectonic evolution of the orogenic belt in the region located between Kerman and Neyriz. *Journal of Asian Earth Sciences*, 24(4), 405-417. https://doi.org/10.1016/j.jseaes.2003.11.007.

Stead D., Wolter A. (2015). A critical review of rock slope failure mechanisms: the importance of structural geology. *Journal of Structural Geology*, 74, 1-23. https://doi.org/10.1016/j.jsg.2015.02.002.

Stern R.J., Moghadam H.S., Pirouz M., Mooney W. (2021). The geodynamic evolution of Iran. *Annual Review of Earth and Planetary Sciences*, 49(1), 9-36. https://doi.org/10.1146/annurev-earth-071620-052109.

Stöcklin J. (1968). Structural history and tectonics of Iran: a review. *AAPG Bulletin*, 52(7), 1229-1258.

Tadayon M., Rossetti F., Zattin M., Nozaem R., Calzolari G., Madanipour S., Salvini F. (2017). The post-Eocene evolution of the Doruneh Fault region (central Iran): The intraplate response to the Reorganization of the Arabia-Eurasia collision zone. *Tectonics*, 36(12), 3038-3064. https://doi.org/10.1002/2017TC004595.

Tan Y.J., Waldhauser F., Ellsworth W.L., Zhang M., Zhu W., Michele M., Segou M. (2021). Machine-learning-based high-resolution earthquake catalog reveals how complex fault structures were activated during the 2016–2017 central Italy sequence. *The Seismic Record*, 1(1), 11-19. https://doi.org/10.1785/0320210001.

Torabi A., Berg S.S. (2011). Scaling of fault attributes: A review. *Marine and Petroleum Geology*, 28(8), 1444-1460. https://doi.org/10.1016/j.marpetgeo.2011.04.003.

Twiss, R.J., Moores E.M. (2006). *Structural Geology (2nd Edition)*. W.H.Freeman & Co Ltd, New York, USA.

Ulusay R., Aydan Ö., Hamada M. (2002). The behaviour of structures built on active fault zones: examples from the recent earthquakes of Turkey. *Structural Engineering/Earthquake Engineering*, 19(2), 149s-167s.

Walker R., Jackson J. (2004). Active tectonics and late Cenozoic strain distribution in central and eastern Iran. *Tectonics*, 23(5), TC5010. https://doi.org/10.1029/2003TC001529.

Walker R.T., Talebian M., Saiffori S., Sloan R.A., Rasheedi A., MacBean N., Ghassemi A. (2010). Active faulting, earthquakes, and restraining bend development near Kerman city in southeastern Iran. *Journal of Structural Geology*, 32(8), 1046-1060. https://doi.org/10.1016/j.jsg.2010.06.012.

Walpersdorf A., Manighetti I., Mousavi Z., Tavakoli F., Vergnolle M., Jadidi A., Sedigh, M. (2014). Present-day kinematics and fault slip rates in eastern Iran, derived from 11 years of GPS data. *Journal of Geophysical Research: Solid Earth*, 119(2), 1359-1383. https://doi.org/10.1002/2013JB010620.

Yamaji A. (2000). The multiple inverse method applied to meso-scale faults in mid-Quaternary fore-arc sediments near the triple trench junction off central Japan. *Journal of Structural Geology*, 22(4), 429-440. https://doi.org/10.1016/S0191-8141(99)00162-5.

Zanchi A., Berra F., Mattei M., Ghassemi M.R., Sabouri J. (2006). Inversion tectonics in central Alborz, Iran. *Journal of Structural Geology*, 28(11), 2023-2037. https://doi.org/10.1016/j.jsg.2006.06.020.

Zhang S., Yang K., Cao Y. (2018). GIS-based rapid disaster loss assessment for earthquakes. *IEEE Access*, 7, 6129-6139. https://doi.org/10.1109/ACCESS.2018.2889918.